

# Effects of nucleon resonances on $\eta$ photoproduction off the neutron reexamined

Jung-Min Suh,<sup>1,\*</sup> Sang-Ho Kim,<sup>2,3,†</sup> and Hyun-Chul Kim<sup>1,4,5,‡</sup>

<sup>1</sup>*Department of Physics, Inha University, Incheon 22212, Republic of Korea*

<sup>2</sup>*Center for Extreme Nuclear Matters (CENuM),*

*Korea University, Seoul 02841, Republic of Korea*

<sup>3</sup>*Department of Physics, Pukyong National University (PKNU), Busan 48513, Republic of Korea*

<sup>4</sup>*Advanced Science Research Center, Japan Atomic Energy Agency, Shirakata, Tokai, Ibaraki, 319-1195, Japan*

<sup>5</sup>*School of Physics, Korea Institute for Advanced Study (KIAS), Seoul 02455, Republic of Korea*

(Dated: October 12, 2018)

We investigate  $\eta$  photoproduction off the neutron target, i.e.,  $\gamma n \rightarrow \eta n$ , employing an effective Lagrangian method combining with a Regge approach. As a background, we consider nucleon exchange in the  $s$ -channel diagram and  $\rho$ - and  $\omega$ -meson Regge trajectories in the  $t$  channel. The role of nucleon resonances given in the Review of Particle Data Group in the range of  $W \approx 1500 - 2100$  MeV and the narrow nucleon resonance  $N(1685, 1/2^+)$  is extensively studied. The numerical results of the total and differential cross sections, double polarization observable  $E$ , and helicity-dependent cross sections  $\sigma_{1/2}$ ,  $\sigma_{3/2}$  are found to be in qualitative agreement with the recent A2 experimental data. The predictions of the beam asymmetry are also given.

Keywords:  $\eta$  photoproduction off the neutron, narrow nucleon resonances, effective Lagrangian approach,  $t$ -channel Regge trajectories

arXiv:1810.05056v1 [hep-ph] 11 Oct 2018

---

\* E-mail: suhjungmin@inha.edu

† E-mail: sangho\_kim@korea.ac.kr

‡ E-mail: hchkim@inha.ac.kr

## I. INTRODUCTION

Photoproduction of mesons provides an essential tool to investigate excited baryons. In particular,  $\eta$  photoproduction plays a role of a filter for excited nucleon resonances, since  $\eta$  is a pseudoscalar and isoscalar meson, and it contains hidden strangeness. So, only the selected number of the excited nucleon resonances can be exclusively studied, which can be only coupled to the  $\eta$  meson [1]. Since Kuznetsov et al. [2] reported the evidence of the narrow bump-like structure around the center-of-mass (CM) energy  $W \sim 1.68$  GeV in  $\eta$  photoproduction off the quasi-free neutron, a number of experiments on  $\eta$  photoproduction off the neutron has been performed by the Tohoku group at the Laboratory of Nuclear Science (LNS) at Tohoku University [3], CBELSA/TAPS Collaboration [4–6], and A2 Collaboration [7–9]. Starting from the  $\eta N$  threshold, the total cross section of  $\eta$  photoproduction off the nucleon raises rapidly because of the dominant and broad excited nucleon resonance  $N(1535, 1/2^-)$ . It falls off somewhat slowly from  $W \sim 1535$  MeV. The narrow bump-like structure is then observed on the shoulder of the  $N(1535, 1/2^-)$  in the vicinity of  $W \sim 1.68$  GeV but only in  $\eta$  photoproduction off the neutron. Such a narrow structure was not found in the proton target as reported by Refs. [4, 10] or a dip-like structure appears [5, 11]. The finding that the narrow bump-like structure is only clearly seen in  $\eta$  photoproduction off the neutron is coined *neutron anomaly* [12].

Theoretical interpretations on this narrow bump-like structure are not in consensus, whereas the evidence of its existence has been firmly established. Right after the finding of it, Refs. [13–15] explained the  $\gamma n \rightarrow \eta n$  reaction very well within an Effective Lagrangian approach, regarding the narrow structure as the narrow nucleon resonance  $N(1685, 1/2^+)$ . These works were motivated by the results from the chiral quark-soliton model ( $\chi$ QSM) [16, 17]. We want to mention that recently, A2 Collaboration has carried out the measurement of the double polarization observables and the helicity-dependent cross sections for  $\eta$  photoproduction from the quasi-free proton and neutron [18, 19]. Interestingly, the narrow bump-like structure was seen only in the spin-1/2 helicity-dependent cross section. A narrow structure is experimentally favored to be interpreted as a narrow  $P_{11}$  nucleon resonance as mentioned by Ref. [18], which supports the analyses of Refs. [13–15]. On the other hand, there have been various theoretical disputes on the interpretation of the narrow bump-like structure as a narrow  $N(1685, 1/2^+)$  resonance. Ref. [20] proposed as the nature of the narrow structure the coupled-channel effects by  $N(1650, 1/2^-)$  and  $N(1710, 1/2^+)$  within the unitary coupled-channels effective Lagrangian approach. Reference [21] considered it as the interference effects of  $N(1535, 1/2^-)$ ,  $N(1650, 1/2^-)$ ,  $N(1710, 1/2^+)$ , and  $N(1720, 3/2^+)$  resonance contributions, based on a coupled-channels  $K$ -matrix method. The Bonn-Gatchina partial-wave analysis (Bn-Ga PWA) group [22–24] regarded the narrow bump-like structure as the effects arising from interference between  $N(1535, 1/2^-)$  and  $N(1650, 1/2^-)$ . The Bn-Ga PWA group argued that the inclusion of the narrow nucleon resonance made the results worse within their PWA approach. On the other hand, Döring and Nakayama [25] examined the ratio of the cross section  $\sigma_n/\sigma_p$  with the intermediate meson-baryon states with strangeness and considered the narrow structure as the effects coming from the opening of the strangeness channel in intermediate states. Kuznetsov et al. [12, 26, 27] rebutted that interpretation of the narrow bump-like structure as an interference effect between the  $S$ -wave nucleon resonances. Moreover, both the narrow excited proton and neutron were also seen in Compton scattering  $\gamma N \rightarrow \gamma N$  [28, 29] and the reactions  $\gamma N \rightarrow \pi \eta N$  [30].

Meanwhile, two of the authors recently studied  $K^0 \Lambda$  photoproduction off the neutron based on an effective Lagrangian approach combined with a Regge model [31]. They found that the narrow resonance  $N(1685, 1/2^+)$  comes into critical play to describe the experimental data on the differential cross sections. The corresponding CLAS data show a dip structure in forward angle regions at the pole position of the narrow nucleon resonance, although the signs are not clear since the width of the dip is not as large as the energy bin of the data [32]. On the other hand, a different conclusion was drawn by the Bn-Ga PWA group [33] with the same CLAS data, in which the evidence of the  $N(1685, 1/2^+)$  was discarded. Note that this dip structure was not observed experimentally in  $K^+ \Lambda$  photoproduction, although there are relevant theoretical studies to support its existence [34, 35].

In view of this puzzled situation related to the existence of  $N(1685, 1/2^+)$ , we want to reexamine  $\eta$  photoproduction off the neutron within the framework of the effective Lagrangian approach combined with a Regge model, focusing on the role of  $N(1685, 1/2^+)$ . Since the previous works [13, 14] were performed by using old experimental information on the excited nucleon resonances and more experimental data on the narrow  $N(1685, 1/2^+)$  resonances were compiled as explained above, it is worthwhile to reinvestigate the roles of the excited nucleon resonances in  $\eta$  photoproduction off the neutron with  $N(1685, 1/2^+)$  also included as a nucleon resonance. We include altogether sixteen different excited nucleon resonances in the  $s$  channel, fixing all relevant parameters by using the experimental data and empirical information. Each contribution of the excited nucleons will be scrutinized. The  $t$  channel will be described by vector Reggeon exchanges.

This paper is organized as follows: In Section II we explain the general formalism of the effective Lagrangian approach together with the Regge model in detail. In Section III, we present the numerical results of the total and differential cross sections, and the double polarization observables for the  $\gamma n \rightarrow \eta n$  reaction and discuss physical implications of them. Section IV is devoted to summary and outlook.

## II. GENERAL FORMALISM

In this paper, we study  $\eta$  photoproduction off the neutron in an effective Lagrangian approach with a Regge method. The scattering amplitudes for this process can be divided into two parts, i.e., the background and excited nucleon resonance ( $N^*$ ) contributions. Firstly, we consider  $\rho$  and  $\omega$  Reggeon exchanges in the  $t$  channel as the background contribution that are shown in Fig. 1(a) in which the symbols in parentheses stand for the four-momenta of the corresponding particles. These two vector-Reggeon exchanges are enough to describe the  $\gamma n \rightarrow \eta n$  reaction at higher energies.  $N$  exchanges in both the  $s$  (Fig. 1(b)) and  $u$  (Fig. 1(c)) channels are also taken into account as the background contributions, although their effects are tiny on the cross sections. Secondly, the  $N^*$  contributions are included in the  $s$ -channel diagram in addition to nucleon exchange (Fig. 1(b)), of which information is taken from the Review of Particle Physics [1]. In the present work, we introduce fifteen nucleon resonances that are coupled strongly to the  $\gamma N$  and  $\eta N$  vertices. We regard the narrow bump-like structure as the narrow resonance  $N(1685, 1/2^+)$  of which the existence was predicted in the  $\chi$ QSM [16, 17].

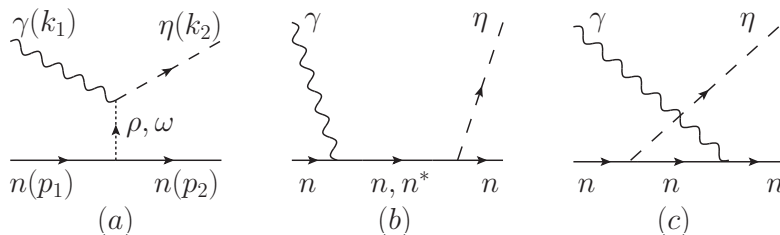


FIG. 1. Feynman diagrams for the  $\gamma n \rightarrow \eta n$  reaction.

We start with the background contributions. The photon vertices can be constructed by using the following effective Lagrangians

$$\begin{aligned} \mathcal{L}_{\gamma\eta V} &= \frac{eg_{\gamma\eta V}}{4M_\eta} \epsilon^{\mu\nu\alpha\beta} F_{\mu\nu} V_{\alpha\beta} \phi_\eta + \text{H.c.}, \\ \mathcal{L}_{\gamma NN} &= -\bar{N} \left[ e_N \gamma_\mu - \frac{e\kappa_N}{2M_N} \sigma_{\mu\nu} \partial^\nu \right] A^\mu N, \end{aligned} \quad (1)$$

where  $F_{\mu\nu}$  and  $V_{\alpha\beta}$  denotes the electromagnetic and vector-meson field-strength tensors defined respectively by  $F_{\mu\nu} = \partial_\mu A_\nu - \partial_\nu A_\mu$  and  $V_{\alpha\beta} = \partial_\alpha V_\beta - \partial_\beta V_\alpha$ .  $A_\mu$ ,  $\phi_\eta$ , and  $N$  stand for the photon, pseudoscalar  $\eta$  meson, and nucleon fields, respectively.  $V$  represents generically either the  $\rho$ - or  $\omega$ -vector mesons.  $M_h$  is the mass of the hadron  $h$  involved in the process.  $e_N$  designates the electric charge and  $e$  the unit electric charge. In the present work, we need to consider only the magnetic part in the  $\gamma NN$  vertex because the charge of the  $\eta$  meson is neutral. The coupling constant  $g_{\gamma\eta V}$  is extracted from the experimental data on the corresponding decay width of the vector meson  $V$

$$\Gamma_{V \rightarrow \eta\gamma} = \frac{g_{\gamma\eta V}^2}{12\pi} \frac{e^2}{M_\eta^2} \left( \frac{M_V^2 - M_\eta^2}{2M_V} \right)^3. \quad (2)$$

Since the decay widths of the  $\rho$  and  $\omega$  mesons are experimentally known to be  $\Gamma_{\rho \rightarrow \eta\gamma} = 45.5$  keV and  $\Gamma_{\omega \rightarrow \eta\gamma} = 3.82$  keV [1], one can easily determine the vector coupling constants as follows

$$g_{\rho\eta\gamma} = 0.91, \quad g_{\omega\eta\gamma} = 0.24. \quad (3)$$

The anomalous magnetic moment of the neutron is also given by the PDG [1]:  $\kappa_n = -1.91$ .

The effective Lagrangians for the meson-nucleon interactions are written as

$$\begin{aligned} \mathcal{L}_{VNN} &= -g_{VNN} \bar{N} \left[ \gamma_\mu N - \frac{\kappa_{VNN}}{2M_N} \sigma_{\mu\nu} N \partial^\nu \right] V^\mu + \text{H.c.}, \\ \mathcal{L}_{\eta NN} &= \frac{g_{\eta NN}}{2M_N} \bar{N} \gamma_\mu \gamma_5 N \partial^\mu \phi_\eta. \end{aligned} \quad (4)$$

The relevant strong coupling constants are taken from the Nijmegen soft-core potential [36]

$$g_{\rho NN} = 2.97, \quad \kappa_{\rho NN} = 4.22, \quad g_{\omega NN} = 10.4, \quad \kappa_{\omega NN} = 0.41, \quad g_{\eta NN} = 6.34. \quad (5)$$

In order to construct the invariant amplitude for vector-Reggeon exchange, We follow the Regge formalism of Refs. [37, 38]. In general, the Regge amplitude is obtained by replacing the Feynman propagators by the Regge propagators as follows

$$\frac{1}{t - M_V^2} \rightarrow P_V^{\text{Regge}}(t) = \left(\frac{s}{s_0}\right)^{\alpha_V(t)-1} \frac{1}{\sin[\pi\alpha_V(t)] \Gamma[\alpha_V(t)]} D_V(t). \quad (6)$$

We fix the energy-scale parameter to be  $s_0 = 1 \text{ GeV}^2$  for simplicity. To determine the signature factor  $D_V(t)$ , we refer to pion photoproduction  $\gamma p \rightarrow \pi^0 p$  [38], where the same Regge trajectories are considered in the  $t$ -channel. It is demonstrated that the  $\rho$ -meson trajectory should be degenerate to describe the proper asymptotic high-energy behavior whereas the  $\omega$  trajectory is nondegenerate to explain the dip structure for the  $d\sigma/dt$  at a certain point. The signature factors are explicitly expressed as

$$D_\rho(t) = \exp(-i\pi\alpha_\rho(t)), \quad D_\omega(t) = \frac{\exp(-i\pi\alpha_\omega(t)) - 1}{2}, \quad (7)$$

and the vector-meson Regge trajectories read [38]

$$\alpha_\rho(t) = 0.55 + 0.8t, \quad \alpha_\omega(t) = 0.44 + 0.9t. \quad (8)$$

Note that the invariant amplitudes for these background parts are all separately gauge invariant by construction.

To respect the finite sizes of hadrons involved, we need to introduce the empirical form factors. We mention that the form factors are in effect main sources for model uncertainties. We use the following type of the form factors for  $N$  exchange in the  $s$  channel:

$$F_N(q^2) = \frac{\Lambda^4}{\Lambda^4 + (q^2 - M_N^2)^2}, \quad (9)$$

where  $q^2$  is the squared momentum of  $q_s = k_1 + p_1$  or  $q_u = p_2 - k_1$ . In the case of the  $t$ -channel Reggeon exchange, we introduce a scale factor which plays a role of the form factor:

$$C_V(t) = \frac{a}{(1 - t/\Lambda^2)^2}. \quad (10)$$

In the present work, we use the fixed values of the cut-off masses  $\Lambda_N = 1.0 \text{ GeV}$  to avoid additional ambiguities. The scaling parameters are taken to be  $a_{\rho,\omega} = 1.4$  and  $\Lambda_{\rho,\omega} = 1.0 \text{ GeV}$ .

There are many excited nucleon resonances above the  $\eta N$  threshold [1], among which we select fifteen  $N^*$ s in the range of  $W \approx (1500 - 2100) \text{ MeV}$  as listed in Table I. Note that  $N(1990, 7/2^+)$ ,  $N(2040, 3/2^+)$ ,  $N(2060, 5/2^-)$  and  $N(2100, 1/2^+)$  are excluded because of lack of information as to how they are coupled to the photon or the  $\eta$  meson. In addition to the fifteen nucleon resonances, we consider the narrow resonance  $N(1685, 1/2^+)$ . The effective Lagrangians for the photo-excitations  $\gamma N \rightarrow N^*$  are given in the following forms:

$$\begin{aligned} \mathcal{L}_{\gamma NN^*}^{1/2^\pm} &= \frac{eh_1}{2M_N} \bar{N}\Gamma^\mp \sigma_{\mu\nu} \partial^\nu A^\mu N^* + \text{H.c.}, \\ \mathcal{L}_{\gamma NN^*}^{3/2^\pm} &= -ie \left[ \frac{h_1}{2M_N} \bar{N}\Gamma_\nu^\pm - \frac{ih_2}{(2M_N)^2} \partial_\nu \bar{N}\Gamma^\pm \right] F^{\mu\nu} N_\mu^* + \text{H.c.}, \\ \mathcal{L}_{\gamma NN^*}^{5/2^\pm} &= e \left[ \frac{h_1}{(2M_N)^2} \bar{N}\Gamma_\nu^\mp - \frac{ih_2}{(2M_N)^3} \partial_\nu \bar{N}\Gamma^\mp \right] \partial^\alpha F^{\mu\nu} N_{\mu\alpha}^* + \text{H.c.}, \\ \mathcal{L}_{\gamma NN^*}^{7/2^\pm} &= ie \left[ \frac{h_1}{(2M_N)^3} \bar{N}\Gamma_\nu^\pm - \frac{ih_2}{(2M_N)^4} \partial_\nu \bar{N}\Gamma^\pm \right] \partial^\alpha \partial^\beta F^{\mu\nu} N_{\mu\alpha\beta}^* + \text{H.c.}, \end{aligned} \quad (11)$$

where the superscripts denote the spin and parity of the corresponding nucleon resonances.  $N^*$  stands for the spin-1/2 excited nucleon field whereas  $N_\mu^*$ ,  $N_{\mu\alpha}^*$ , and  $N_{\mu\alpha\beta}^*$  represent the Rarita-Schwinger fields of spin-3/2, -5/2, and -7/2, respectively.  $\Gamma^\pm$  and  $\Gamma_\nu^\pm$ , which are related to the parity of an excited nucleon involved, are defined by

$$\Gamma^\pm = \begin{pmatrix} \gamma_5 \\ I_{4 \times 4} \end{pmatrix}, \quad \Gamma_\nu^\pm = \begin{pmatrix} \gamma_\nu \gamma_5 \\ \gamma_\nu \end{pmatrix}. \quad (12)$$

To determine the magnetic transition moments  $h_{1,2}$ , we relate them to the Breit-Wigner helicity amplitudes  $A_{1/2,3/2}$  [39, 40]. The  $A_{1/2,3/2}$  are taken from the PDG [1]. Some ambiguities are contained in  $A_{1/2,3/2}$ . In the

present work, we choose the central values of them. Although we could obtain better theoretical results by fitting these couplings, we would not perform it because the purpose of this work is to investigate how far we can describe the experimental data when the narrow  $N^*(1685, 1/2^+)$  is explicitly included. Thus, in the procedure, it is essential to reduce any theoretical ambiguities such that the contribution of this narrow nucleon resonance can be carefully examined. All the relevant the helicity amplitudes and the photo-coupling constants are summarized in Table I. The magnetic transition moment of the narrow resonance  $N(1685, 1/2^+)$  is taken from Ref. [41].

TABLE I. The fifteen nucleon resonances taken from the PDG [1] and the numerical values of the magnetic transition moments. The helicity amplitudes  $A_{1/2, 3/2}$  are given in units of  $10^{-3}/\sqrt{\text{GeV}}$ . In addition, we include the narrow nucleon resonance  $N(1685, 1/2^+)$ .

State	Rating	Width [MeV]	$A_{1/2}$	$A_{3/2}$	$h_1$	$h_2$
$N(1520, 3/2^-)$	****	100-120 (110)	$\approx -50$	$\approx -115$	-0.77	-0.62
$N(1535, 1/2^-)$	****	125-175 (140)	$\approx -75$	...	-0.53	...
$N(1650, 1/2^-)$	****	100-150 (125)	$\approx -10$	...	0.063	...
$N(1675, 5/2^-)$	****	130-160 (145)	$-60 \pm 5$	$-85 \pm 10$	4.88	5.45
$N(1680, 5/2^+)$	****	100-135 (120)	$\approx 30$	$\approx -35$	...	...
$N(1700, 3/2^-)$	***	100-300 (200)	$25 \pm 10$	$-32 \pm 18$	-1.43	1.64
$N(1710, 1/2^+)$	****	80-200 (140)	$-40 \pm 20$	...	0.24	...
$N(1720, 3/2^+)$	****	150-400 (250)	$-80 \pm 50$	$-140 \pm 65$	1.50	1.61
$N(1860, 5/2^+)$	**	300	$21 \pm 13$	$34 \pm 17$	0.28	1.09
$N(1875, 3/2^-)$	***	120-250 (200)	$10 \pm 6$	$-20 \pm 15$	-0.55	0.54
$N(1880, 1/2^+)$	***	200-400 (300)	$-60 \pm 50$	...	0.30	...
$N(1895, 1/2^-)$	****	80-200 (120)	$13 \pm 6$	...	0.067	...
$N(1900, 3/2^+)$	****	100-320 (200)	$0 \pm 30$	$-60 \pm 45$	0.29	-0.56
$N(2000, 5/2^+)$	**	300	$-18 \pm 12$	$-35 \pm 20$	-0.47	-0.56
$N(2120, 3/2^-)$	***	260-360 (300)	$110 \pm 45$	$40 \pm 30$	-1.71	2.41
$N(1685, 1/2^+)$		30			-0.315 [41]	

The effective Lagrangians for the strong vertices  $\eta NN^*$  are expressed as

$$\begin{aligned}
\mathcal{L}_{\eta NN^*}^{1/2^\pm} &= -ig_{\eta NN^*} \phi_\eta \bar{N} \Gamma^\pm N^* + \text{H.c.}, \\
\mathcal{L}_{\eta NN^*}^{3/2^\pm} &= \frac{g_{\eta NN^*}}{M_\eta} \partial^\mu \phi_\eta \bar{N} \Gamma^\mp N^*_\mu + \text{H.c.}, \\
\mathcal{L}_{\eta NN^*}^{5/2^\pm} &= \frac{ig_{\eta NN^*}}{M_\eta^2} \partial^\mu \partial^\nu \phi_\eta \bar{N} \Gamma^\pm N^*_{\mu\nu} + \text{H.c.}, \\
\mathcal{L}_{\eta NN^*}^{7/2^\pm} &= -\frac{g_{\eta NN^*}}{M_\eta^3} \partial^\mu \partial^\nu \partial^\alpha \phi_\eta \bar{N} \Gamma^\mp N^*_{\mu\nu\alpha} + \text{H.c.}
\end{aligned} \tag{13}$$

Though there are more terms in the Lagrangians for higher-spin nucleon resonances, we do not need them, considering the angular momenta and parity conservation of  $\eta$  photoproduction. The magnitude of the strong coupling constants,  $g_{\eta NN^*}$ , can be extracted from the partial decay widths  $\Gamma_{N^* \rightarrow \eta N}$  given by the experimental data of the PDG [1]. However, their signs are unknown and, moreover, only the upper limits are known for some of  $\Gamma_{N^* \rightarrow \eta N}$ . So, we use information on these unknown decay amplitudes from the quark model predictions [42]. To do that, we employ the following relation [31, 43]:

$$\langle \eta(\vec{q}) N(-\vec{q}, m_f) | -i\mathcal{H}_{\text{int}} | N^*(\mathbf{0}, m_j) \rangle = 4\pi M_{N^*} \sqrt{\frac{2}{|\vec{q}|}} \sum_{\ell, m_\ell} \langle \ell m_\ell \frac{1}{2} m_f | j m_j \rangle Y_{\ell, m_\ell}(\hat{q}) G(\ell), \tag{14}$$

where  $\langle \ell m_\ell \frac{1}{2} m_f | j m_j \rangle$  and  $Y_{\ell, m_\ell}(\hat{q})$  are the Clebsch-Gordan coefficients and spherical harmonics, respectively. A partial decay width is then obtained from the decay amplitudes  $G(\ell)$

$$\Gamma(N^* \rightarrow \eta N) = \sum_{\ell} |G(\ell)|^2. \tag{15}$$

The spin and parity of the nucleon resonance impose constraints on the relative orbital angular momentum  $\ell$  of the  $\eta N$  final state. For example, in the cases of  $j^P = \frac{1}{2}^+$  and  $\frac{1}{2}^-$  resonances, only  $p(\ell = 1)$  and  $s(\ell = 0)$  waves are

allowed, respectively. Finally, the relations between the decay amplitudes and the strong coupling constants for the vertices with  $j^P = (1/2^\pm, 3/2^\pm, 5/2^\pm, 7/2^\pm)$  nucleon resonances are derived as follows:

$$\begin{aligned}
G\left(\frac{1+P}{2}\right) &= \mp \sqrt{\frac{|\vec{q}|(E_N \mp M_N)}{4\pi M_{N^*}}} g_{\eta NN^*} \text{ for } N^*(1/2^P), \\
G\left(\frac{3-P}{2}\right) &= \pm \sqrt{\frac{|\vec{q}|^3(E_N \pm M_N)}{12\pi M_{N^*}}} \frac{g_{\eta NN^*}}{M_\eta} \text{ for } N^*(3/2^P), \\
G\left(\frac{5+P}{2}\right) &= \mp \sqrt{\frac{|\vec{q}|^5(E_N \mp M_N)}{30\pi M_{N^*}}} \frac{g_{\eta NN^*}}{M_\eta^2} \text{ for } N^*(5/2^P), \\
G\left(\frac{7-P}{2}\right) &= \pm \sqrt{\frac{|\vec{q}|^7(E_N \pm M_N)}{70\pi M_{N^*}}} \frac{g_{\eta NN^*}}{M_\eta^3} \text{ for } N^*(7/2^P),
\end{aligned} \tag{16}$$

where the magnitude of the three-momentum and the energy for  $N$  in the rest frame of the nucleon resonance are given respectively as

$$|\vec{q}| = \frac{1}{2M_{N^*}} \sqrt{[M_{N^*}^2 - (M_N + M_\eta)^2][M_{N^*}^2 - (M_N - M_\eta)^2]}, \quad E_N = \sqrt{M_N^2 + |\vec{q}|^2}. \tag{17}$$

In Table II, the relevant values for the strong decays are tabulated.  $\Gamma_{N^*}$  designates the decay width of  $N^*$ . We use the values in parentheses in Table I for them. For the spin-3/2, -5/2, and -7/2 propagators, we employ the Rarita-Schwinger formalism [44–47] as in Refs. [39, 40, 48–50]. The off-shell terms of the Rarita-Schwinger fields are excluded. The PDG data are only available for the three nucleon resonances above 1875 MeV, i.e.,  $N(1880, 1/2^+)$ ,  $N(1895, 1/2^-)$ , and  $N(1900, 3/2^+)$ , we determine the signs of the corresponding strong coupling constants phenomenologically. The numerical values of all the necessary coupling constants  $g_{\eta NN^*}$  are listed in the last column of Table II.

TABLE II. The numerical values of the strong couplings of the nucleon resonances. The decay amplitudes  $G(\ell)$  in units of MeV are obtained from Ref. [42] and the branching ratios of  $N^* \rightarrow \eta N$  decays are taken from Ref. [1].

State	$G(\ell)$	$g_{\eta NN^*}$	$\Gamma_{N^* \rightarrow \eta N} / \Gamma_{N^*} [\%]$	$ g_{\eta NN^*} $	$g_{\eta NN^*}$ (final)
$N(1520, 3/2^-)$	$0.4_{-0.4}^{+2.9}$	-8.30	0.07 – 0.09	5.23 – 6.49	-5.23
$N(1535, 1/2^-)$	$8.1 \pm 0.8$	2.05	30 – 55	1.58 – 2.14	2.10
$N(1650, 1/2^-)$	$-2.4 \pm 1.6$	-0.43	15 – 35	0.76 – 1.16	-0.80
$N(1675, 5/2^-)$	$-2.5 \pm 0.2$	-2.50	< 1	< 0.90	-0.90
$N(1680, 5/2^+)$	$0.6 \pm 0.1$	-2.98	< 1	< 4.07	-2.47
$N(1700, 3/2^-)$	$-0.2 \pm 0.1$	0.38	seen		0.38
$N(1710, 1/2^+)$	$5.7 \pm 0.3$	-4.23	10 – 50	2.93 – 6.55	-4.00
$N(1720, 3/2^+)$	$5.7 \pm 0.3$	2.08	1 – 5	0.43 – 4.50	1.00
$N(1860, 5/2^+)$	$1.9 \pm 0.8$	-2.84	2 – 6	2.47 – 4.27	-2.47
$N(1875, 3/2^-)$	$4.0 \pm 0.2$	-3.58	< 1	< 0.89	-0.80
$N(1880, 1/2^+)$			5 – 55	2.02 – 6.69	2.00
$N(1895, 1/2^-)$			15 – 40	0.60 – 0.99	0.60
$N(1900, 3/2^+)$			2 – 14	0.33 – 0.87	0.33
$N(2000, 5/2^+)$	$1.9 \pm 0.8$	-1.57	< 4	< 0.90	-0.50
$N(2120, 3/2^-)$	$4.0 \pm 0.2$	-1.91			-1.91
$N(1685, 1/2^+)$					1.4

We want to mention that the experimental data on the nucleon resonances in the 2012 edition of the PDG [51] were much changed from those in the 2010 edition [52]. The  $J^P = 5/2^+$  state  $F_{15}(2000)$  is split into  $N(1860, 5/2^+)$  and  $N(2000, 5/2^+)$ . The  $D_{13}(2080)$  is split into  $N(1875, 3/2^-)$  and  $N(2120, 3/2^-)$ . The  $S_{11}(2090)$  is changed into  $N(1895, 1/2^-)$  and the  $N(2060, 5/2^-)$  was previously known as  $D_{15}(2200)$ . The quark model predictions for the decay amplitudes [42] are obtained from the nucleon resonances before the 2012 edition of the PDG. Thus we continue to compute the observables of  $\eta$  photoproduction off the neutron on the assumption that the quark model can reliably produce the values of the decay amplitudes.

For the  $s$ -channel diagrams with the higher-spin nucleon resonances, we introduce the gaussian form factor that can suppress sufficiently the cross sections when the energy grows [53, 54]

$$F_{N^*}(s) = \exp \left\{ -\frac{(s - M_{N^*}^2)^2}{N_{N^*}^4} \right\}. \tag{18}$$

Note that the phase factors for the nucleon resonance cannot be determined just by symmetries, so that we will choose them phenomenologically. The corresponding invariant amplitudes are written by

$$\mathcal{M}_{\text{Res}} = \sum_{N^*} e^{i\psi_{N^*}} \mathcal{M}_{N^*} F_{N^*}(s). \quad (19)$$

We use the the values of the cutoff mass  $\Lambda_{N^*} = 1.0$  GeV again to avoid any additional ambiguities. The phase factor is chosen to be  $e^{i\psi_{N^*}} = e^{i\pi/2}$ .

### III. RESULTS AND DISCUSSIONS

We are now in a position to discuss the present numerical results for the  $\gamma n \rightarrow \eta n$  reaction. In the left panel of Fig. 2, the total cross section is plotted as a function of the CM energy  $W$ . Though we do not display explicitly the contribution of Reggeon-exchanges,  $\rho$ -Reggeon exchange is in fact the strongest one among the background contributions ( $N$ ,  $\rho$ -, and  $\omega$ -Reggeon exchanges). This can be easily understood from the fact that both the  $\rho$ -meson radiative and strong coupling constants are larger than those of the nucleon and  $\omega$  meson (see Eqs. (3) and (5)). However, the effects of the background contributions turn out to be rather small on the total cross section. Even at relatively high energies ( $1.7 \text{ GeV} \leq W \leq 1.9 \text{ GeV}$ ), the magnitudes of the background contributions reach only the level of around 30% compared to the total result. On the other hand, the nucleon resonances play crucial roles of describing the total cross section through the whole energy region from threshold up to  $W = 1.9$  GeV. The present result is in good agreement with the data of the A2 Collaboration [9].

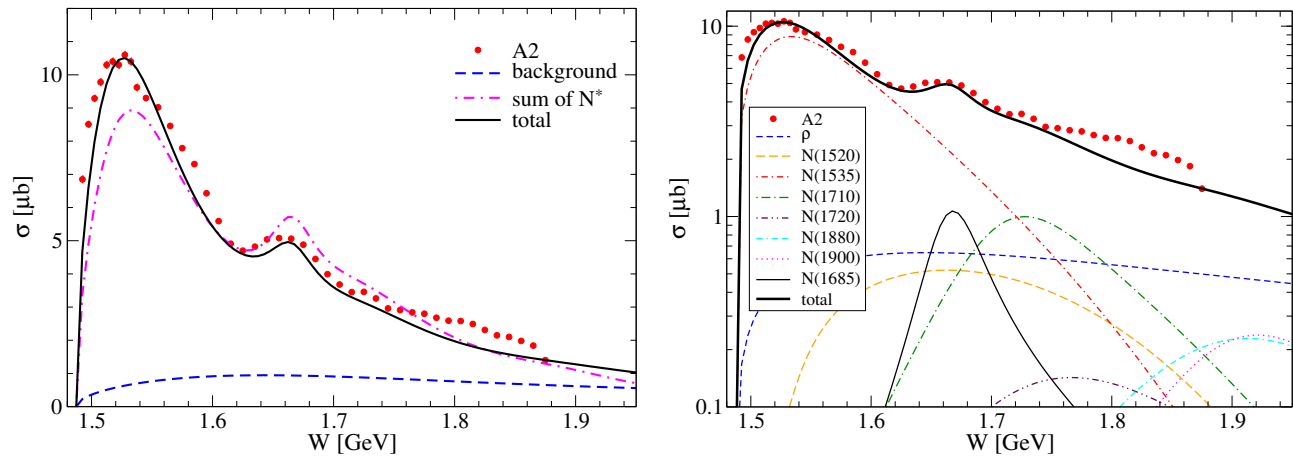


FIG. 2. Total cross section for the  $\gamma n \rightarrow \eta n$  reaction as a function of  $W$ . The left panel draws the numerical result of the present work. The dashed curve represents the background contributions from the nucleon,  $\omega$ -, and  $\rho$ -meson trajectories, whereas the dot-dashed curve draws the contribution of the nucleon resonances. The solid curve plots the total contribution. The right panel depicts each contribution of the exchanged particles to the total cross section for the  $\gamma n \rightarrow \eta n$ . The legend in the box indicates each contribution in a different colored curve. The experimental data are taken from the A2 Collaboration [9].

The right panel of Fig. 2 draws each contribution of the  $\rho$ -Reggeon exchange and the excited nucleon resonances to the total cross section in the logarithmic scale. Note that the contributions of the only seven nucleon resonances are presented, since all other nucleon resonances contribute almost negligibly to the total cross section. As explained in the previous Section, we consider a total of fifteen nucleon resonances from the PDG [1] and in addition the narrow resonance  $N(1685, 1/2^+)$ . It turns out that  $N(1535, 1/2^-)$  is predominantly responsible for the description of the total cross section and  $N(1520, 3/2^-)$  and  $N(1710, 1/2^+)$  also have sizable effects on it. On the other hand,  $N(1720, 3/2^+)$ ,  $N(1880, 1/2^+)$ , and  $N(1900, 3/2^+)$  make rather small contributions to the results of the total cross section. It is very interesting to see that the narrow resonance  $N(1685, 1/2^+)$  indeed describes the narrow bump-like structure around  $W \sim 1.68$  GeV. Though we have not shown the contributions of other nucleon resonances that affect the total cross section negligibly, we will examine their effects on polarization observables later. It is worth to compare our results with other model results. The new version of the EtaMAID model [55] involves the analysis of the  $\gamma n \rightarrow \eta n$  reaction and reaches a different conclusion from the present one. It is demonstrated that besides the dominant  $N(1535, 1/2^-)$ ,  $N(1700, 3/2^-)$ ,  $N(1710, 1/2^+)$ ,  $N(1720, 3/2^+)$ ,  $N(1880, 1/2^+)$ , and  $N(1895, 1/2^-)$  make important contributions to the cross sections. That is, the narrow structure is explained without introducing  $N(1685, 1/2^+)$  but by the interference between other  $s$ ,  $p$ , and  $d$  waves. This interpretation is also distinguished from Ref. [33].

The value of the coupling constant  $g_{\eta NN(1685,1/2^+)}$  is fitted to be 1.4 in our treatment of  $\eta n$  photoproduction to reproduce the A2 data [7]. It corresponds to the branching ratio  $\text{Br}(N(1685, 1/2^+) \rightarrow \eta N) = 5.5\%$  with  $\Gamma_{N(1685,1/2^+)} = 30$  MeV. In the meanwhile, the following upper limit is extracted from the A2 data [7, 9]

$$\sqrt{\text{Br}(N(1685) \rightarrow \eta N)} A_{1/2}^n < (12.3 \pm 0.8) \times 10^{-3} \text{ GeV}^{-1/2}, \quad (20)$$

which is quite close to the present result, i.e.,  $12.1 \times 10^{-3} \text{ GeV}^{-1/2}$ . It is also of great interest to compute the relative branching ratios of  $\eta N$  and  $K\Lambda$  based on the present model. Together with results from a recent work on  $K^0\Lambda$  photoproduction [31], we obtain

$$\frac{\text{Br}(N(1685) \rightarrow K\Lambda)}{\text{Br}(N(1685) \rightarrow \eta N)} \simeq 0.15, \quad (21)$$

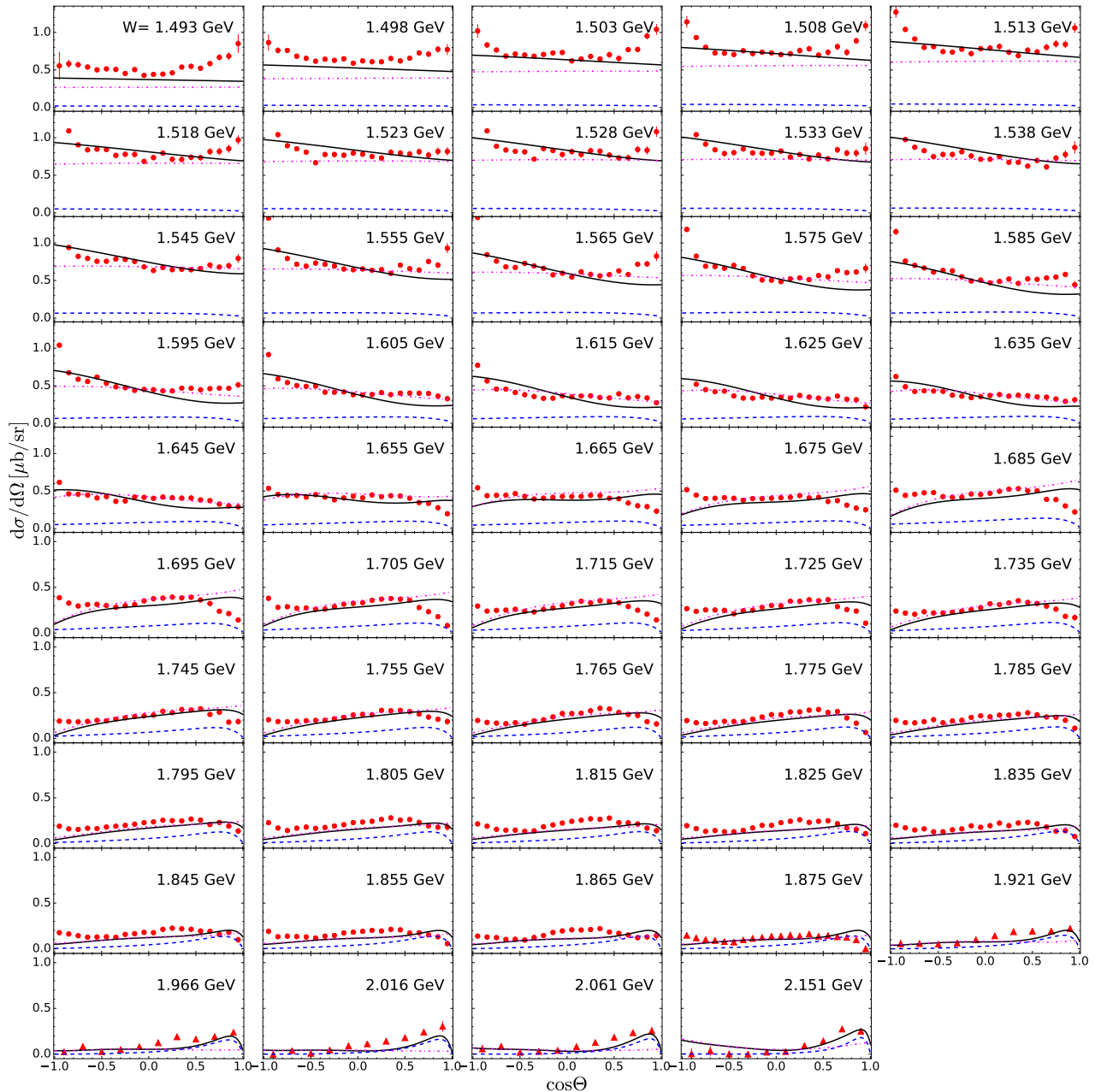


FIG. 3. Differential cross sections for the  $\gamma n \rightarrow \eta n$  as a function of  $\cos\theta$  for each beam energy. The notations are the same as in the left panel of Fig. 2. The data are from the A2 Collaboration (circle) [9] and CBELSA/TAPS Collaboration (triangle) [4].



which is consistent with the yield by a Bn-Ga partial wave analysis, the same experimental data being used [7, 9, 33]:

$$\frac{\text{Br}(N(1685) \rightarrow K\Lambda)}{\text{Br}(N(1685) \rightarrow \eta N)} < \frac{1}{4}. \quad (22)$$

In Fig. 3, the differential cross sections are plotted as a function of  $\cos\theta$  in the range of  $W = 1.5 \text{ GeV} - 2.1 \text{ GeV}$ , where  $\theta$  is the scattering angle of the  $\eta$ -meson in the CM frame. As expected from Fig. 2,  $N^*$  contributions are the most important ones to describe the A2 [9] and CBELSA/TABS [4] data. However, the background contribution also helps to improve the experimental data, especially at higher energies. The effect of the background is small near the threshold but gets larger as photon energy  $W$  increases.

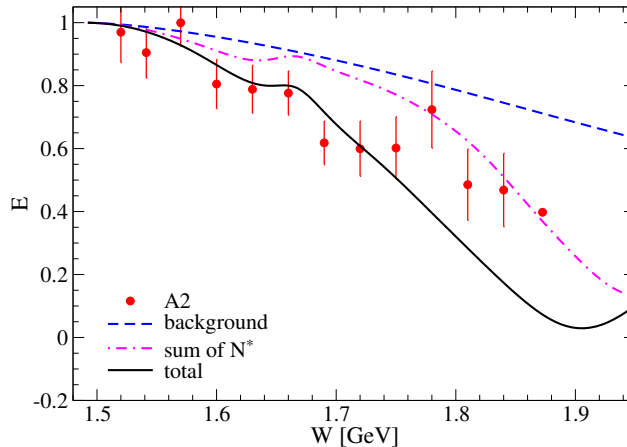


FIG. 4. Double polarization observable  $E$  for the  $\gamma n \rightarrow \eta n$  as a function of  $W$ . The notations are the same as in the left panel of Fig. 2. The data are taken from the A2 Collaboration [18].

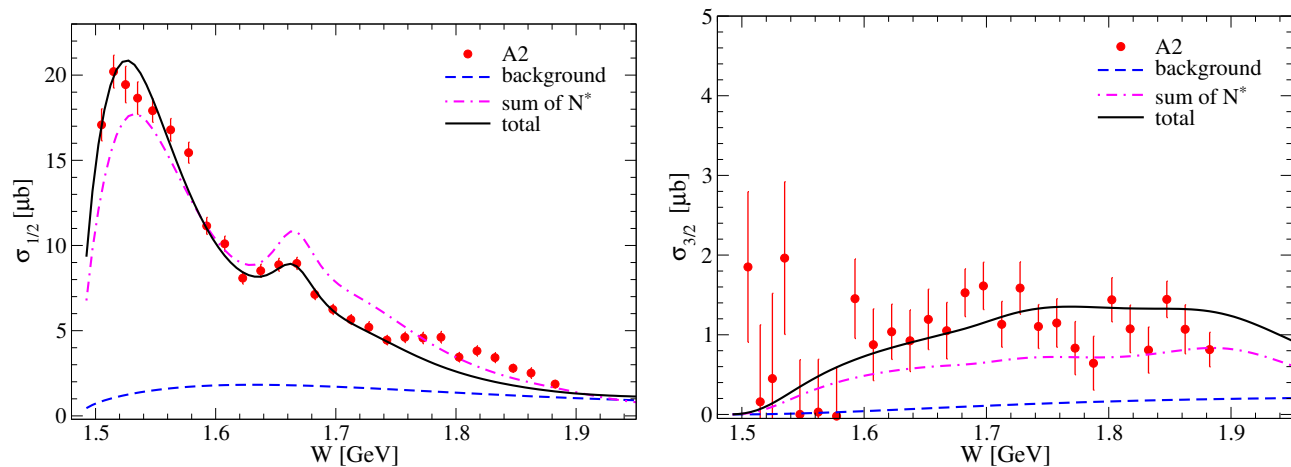


FIG. 5. Helicity-dependent total cross section for the  $\gamma n \rightarrow \eta n$  as a function of  $W$ . The notations are the same as in the left panel of Fig. 2. The data are taken from the A2 Collaboration [18].

Since a number of nucleon resonances are involved in the present model, it is of importance to compute various polarization observables to pin down the role of each nucleon resonance more properly. In Fig. 4, the double polarization observable  $E$  is drawn as a function of  $W$  and compared with the A2 data [18]. It is defined by [18, 56, 57]

$$E = \frac{\sigma^{(r,+z,0)} - \sigma^{(r,-z,0)}}{\sigma^{(r,+z,0)} + \sigma^{(r,-z,0)}} = \frac{\sigma_{1/2} - \sigma_{3/2}}{\sigma_{1/2} + \sigma_{3/2}}, \quad (23)$$

where the superscript  $(B, T, R)$  stands for the polarization state of the photon beam, target nucleon, and recoiled nucleon, respectively. We assume that the reaction takes place in the  $x - z$  plane. Thus the  $+z(-z)$  direction

indicates the incident beam and longitudinally polarized target is parallel (antiparallel) to each other.  $r$  designates the circularly polarized photon beam with helicity  $+1$ . The result of the beam-target asymmetry  $E$  only from the background contribution decreases gradually as the photon energy  $W$  increases and lies above the A2 data. The inclusion of the nucleon resonances pulls down the beam-target asymmetry and it finally reaches zero at  $W = 1.9$  revealing some bump structure near  $W = 1.68$  GeV.

Figure 5 plots the helicity-dependent cross sections  $\sigma_{1/2}$  and  $\sigma_{3/2}$  extracted from the beam-target asymmetry  $E$  [18] and the unpolarized cross section  $\sigma_0$  [9], defined by

$$\sigma_{1/2} = \sigma_0(1 + E), \quad \sigma_{3/2} = \sigma_0(1 - E). \quad (24)$$

The left panel of Fig. 5 clearly shows that the nucleon resonances with spin  $J = 1/2$  is correctly described. The total result is in excellent agreement with the A2 data. More specifically, the background term makes a constructive interference effect with  $N(1535, 1/2^-)$  and a destructive effect with  $N(1685, 1/2^+)$  and  $N(1710, 1/2^+)$ . The result of  $\sigma_{3/2}$  is also in good agreement with the A2 data. The constructive interference effect between the background and resonance contributions is rather important as shown in the right panel of Fig. 5. It indicates that the nucleon resonances with higher spin  $J \geq 3/2$  are properly considered in the present framework. Thus the nucleon resonances with  $J = 3/2$ , i.e.,  $N(1520, 3/2^-)$ ,  $N(1720, 3/2^+)$ , and  $N(1900, 3/2^+)$  come into play for the description of the  $\gamma n \rightarrow \eta n$  in addition to the dominant spin-1/2 nucleon resonances  $N(1535, 1/2^-)$ ,  $N(1685, 1/2^+)$ , and  $N(1710, 1/2^+)$ . The results of Fig. 5 imply that the photo- and strong-coupling constants are well constrained by this model calculations (see Tables I and II).

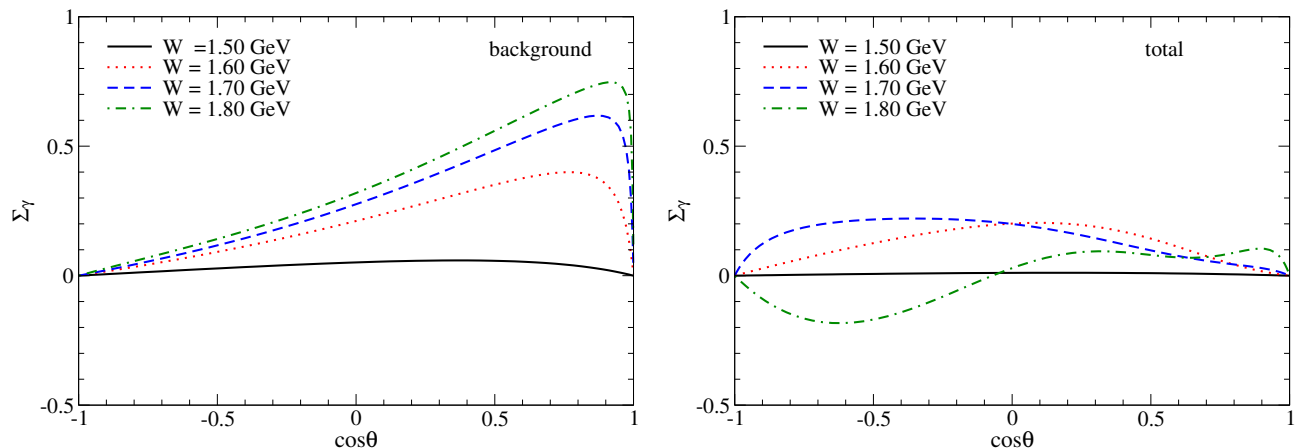


FIG. 6. Beam asymmetry for the  $\gamma n \rightarrow \eta n$  as a function of  $\cos \theta$ .

In Fig. 6, the predictions of the beam asymmetry  $\Sigma_{\bar{\gamma}n \rightarrow \eta n}$  are drawn as a function of  $\cos \theta$  for four different photon energies. It is defined by

$$\Sigma_{\bar{\gamma}n \rightarrow \eta n} = \frac{\frac{d\sigma}{d\Omega}_{\perp} - \frac{d\sigma}{d\Omega}_{\parallel}}{\frac{d\sigma}{d\Omega}_{\perp} + \frac{d\sigma}{d\Omega}_{\parallel}}, \quad (25)$$

where the subscript  $\perp$  means that the photon polarization vector is perpendicular to the reaction plane whereas  $\parallel$  stands for the parallel photon polarization to it. The left panel of Fig. 6 depicts the results of the beam asymmetry only from the background contribution. Because of the dominant vector-meson Regge trajectories, the curves gradually increase as  $\cos \theta$  increases and then falls off drastically at very forward angles. When the nucleon resonances are included as shown in the right panel of Fig. 6, the changes are dramatic. The beam asymmetry gets diminished and the magnitudes of the  $\Sigma_{\bar{\gamma}n \rightarrow \eta n}$  becomes overall equal or less than 0.2. The measurements of the  $\Sigma_{\bar{\gamma}n \rightarrow \eta n}$  as well as other polarization observables by future experiments will become a touchstone to judge which interpretation will turn out right.

#### IV. SUMMARY AND CONCLUSION

In the present work, we investigated  $\eta n$  photoproduction off the neutron taking into account fifteen nucleon resonances from the PDG and in addition the narrow nucleon resonance  $N(1685, 1/2^+)$  in the  $s$ -channel diagram. We

employed an effective Lagrangian approach combining with a Regge model. The  $t$ -channel  $\rho$  and  $\omega$  Regge trajectories and  $N$  exchange in the  $s$  channel are considered as a background. The photo- and strong-coupling constants for the resonance terms were all fixed within the range of values taken from the experimental data and quark model predictions without any complex fitting procedure. We were able to reproduce quantitatively the A2 data for the total and differential cross sections. The branching ratio of the  $N(1685, 1/2^+)$  to the  $\eta N$  channel and the relative branching ratio of it to the  $K\Lambda$  channel were also studied. It turned out that the branching ratio of the  $N(1685, 1/2^+)$  in the  $\eta N$  channel is almost ten times larger than that to the  $K\Lambda$  channel.

The double polarization observables  $E$  and the related helicity-dependent cross sections  $\sigma_{1/2}$  and  $\sigma_{3/2}$  were also examined, since they are useful to clarify the role of spin  $J = 1/2$  and  $J \geq 3/2$  nucleon resonances separately. We have found that  $N(1685, 1/2^+)$  and  $N(1710, 1/2^+)$  are the dominant contributions to the  $\gamma n \rightarrow \eta n$  apart from the  $N(1535, 1/2^-)$  that is the most dominant one. Other nucleon resonances such as  $N(1520, 3/2^-)$ ,  $N(1720, 3/2^+)$ ,  $N(1880, 1/2^+)$ , and  $N(1900, 3/2^+)$  also come into play in describing the A2 data.

### ACKNOWLEDGMENTS

The authors thank D. Werthmüller for providing the A2 experimental data. H.-Ch. K. is grateful to A. Hosaka, T. Maruyama, M. Oka for useful discussions. He wants to express his gratitude to the members of the Advanced Science Research Center at Japan Atomic Energy Agency for the hospitality, where part of the present work was done. This work was supported by the National Research Foundation of Korea (NRF) grant funded by the Korea government(MSIT) (No. 2018R1A5A1025563).

- 
- [1] M. Tanabashi *et al.* (Particle Data Group), Phys. Rev. D **98**, 030001 (2018).
  - [2] V. Kuznetsov *et al.* (GRAAL Collaboration), Phys. Lett. B **647**, 23 (2007).
  - [3] F. Miyahara *et al.*, Prog. Theor. Phys. Suppl. **168**, 90 (2007).
  - [4] I. Jaegle *et al.* (CBELSA and TAPS Collaborations), Phys. Rev. Lett. **100**, 252002 (2008).
  - [5] I. Jaegle *et al.*, Eur. Phys. J. A **47**, 89 (2011).
  - [6] L. Witthauer *et al.* (CBELSA/TAPS Collaboration), Eur. Phys. J. A **53**, 58 (2017).
  - [7] D. Werthmüller *et al.* (A2 Collaboration), Phys. Rev. Lett. **111**, 232001 (2013).
  - [8] L. Witthauer *et al.* (A2 Collaboration), Eur. Phys. J. A **49**, 154 (2013).
  - [9] D. Werthmüller *et al.* (A2 Collaboration), Phys. Rev. C **90**, 015205 (2014).
  - [10] O. Bartalini *et al.* (GRAAL Collaboration), Eur. Phys. J. A **33**, 169 (2007).
  - [11] E. F. McNicoll *et al.* (Crystal Ball at MAMI Collaboration), Phys. Rev. C **82**, 035208 (2010). Erratum: [Phys. Rev. C **84**, 029901 (2011)].
  - [12] V. Kuznetsov *et al.*, Acta Phys. Polon. B **39**, 1949 (2008).
  - [13] K. S. Choi, S. i. Nam, A. Hosaka, and H.-Ch. Kim, Phys. Lett. B **636**, 253 (2006).
  - [14] K. S. Choi, S. i. Nam, A. Hosaka, and H.-Ch. Kim, J. Phys. G **36**, 015008 (2009).
  - [15] A. Fix, L. Tiator, and M. V. Polyakov, Eur. Phys. J. A **32**, 311 (2007).
  - [16] M. V. Polyakov and A. Rathke, Eur. Phys. J. A **18**, 691 (2003).
  - [17] H.-Ch. Kim, M. Polyakov, M. Praszalowicz, G. S. Yang, and K. Goeke, Phys. Rev. D **71**, 094023 (2005).
  - [18] L. Witthauer *et al.* (A2 Collaboration), Phys. Rev. Lett. **117**, 132502 (2016).
  - [19] L. Witthauer *et al.* (A2 Collaboration), Phys. Rev. C **95**, 055201 (2017).
  - [20] V. Shklyar, H. Lenske, and U. Mosel, Phys. Lett. B **650**, 172 (2007).
  - [21] R. Shyam and O. Scholten, Phys. Rev. C **78**, 065201 (2008).
  - [22] A. V. Anisovich, I. Jaegle, E. Klempt, B. Krusche, V. A. Nikonov, A. V. Sarantsev, and U. Thoma, Eur. Phys. J. A **41**, 13 (2009).
  - [23] A. V. Anisovich, E. Klempt, B. Krusche, V. A. Nikonov, A. V. Sarantsev, U. Thoma, and D. Werthmüller, Eur. Phys. J. A **51**, 72 (2015).
  - [24] A. V. Anisovich, V. Burkert, E. Klempt, V. A. Nikonov, A. V. Sarantsev, and U. Thoma, Phys. Rev. C **95**, 035211 (2017).
  - [25] M. Döring and K. Nakayama, Phys. Lett. B **683**, 145 (2010).
  - [26] V. Kuznetsov *et al.*, JETP Lett. **105**, 625 (2017).
  - [27] V. Kuznetsov *et al.*, Pisma Zh. Eksp. Teor. Fiz. **105**, 591 (2017).
  - [28] V. Kuznetsov *et al.*, Phys. Rev. C **83**, 022201(R) (2011).
  - [29] V. Kuznetsov *et al.*, Phys. Rev. C **91**, 042201 (2015).
  - [30] V. Kuznetsov *et al.*, JETP Lett. **106**, 693 (2017) [Pisma Zh. Eksp. Teor. Fiz. **106**, 667 (2017)].
  - [31] S. H. Kim and H.-Ch. Kim, Phys. Lett. B **786**, 156 (2018).
  - [32] N. Compton *et al.*, (CLAS Collaboration), Phys. Rev. C **96**, 065201 (2017).
  - [33] A. V. Anisovich *et al.*, Phys. Rev. C **96**, 055202 (2017).

- [34] T. Mart, Phys. Rev. D **83**, 094015 (2011).
- [35] T. Mart, Phys. Rev. D **88**, 057501 (2013).
- [36] V. G. J. Stoks and Th. A. Rijken, Phys. Rev. C **59**, 3009 (1999); Th. A. Rijken, V. G. J. Stoks, and Y. Yamamoto, *ibid.* **59**, 21 (1999).
- [37] A. Donnachie, H. G. Dosch, P. V. Landshoff, and O. Nachtmann, Pomeron Physics and QCD (Cambridge University Press, UK, 2002).
- [38] M. Guidal, J. M. Laget, and M. Vanderhaeghen, Nucl. Phys. A **627**, 645 (1997).
- [39] Y. Oh, J. Korean Phys. Soc. **59** 3344 (2011).
- [40] Y. Oh, C. M. Ko, and K. Nakayama, Phys. Rev. C **77**, 045204 (2008).
- [41] G. S. Yang and H.-Ch. Kim, arXiv:1809.07489 [hep-ph].
- [42] S. Capstick and W. Roberts, Phys. Rev. D **58**, 074011 (1998).
- [43] S. H. Kim, S. i. Nam, D. Jido, and H.-Ch. Kim, Phys. Rev. D **96**, 014003 (2017).
- [44] R. E. Behrends and C. Fronsdal, Phys. Rev. **106**, 345 (1957).
- [45] J. G. Rushbrooke, Phys. Rev. **143**, 1345 (1966).
- [46] S. J. Chang, Phys. Rev. **161**, 1308 (1967).
- [47] F. A. Berends, J. W. van Holten, P. van Nieuwenhuizen, and B. de Wit, Nucl. Phys. B **154**, 261 (1979).
- [48] S. H. Kim, S. i. Nam, Y. Oh, and H.-Ch. Kim, Phys. Rev. D **84**, 114023 (2011).
- [49] S. H. Kim, S. i. Nam, A. Hosaka, and H.-Ch. Kim, Phys. Rev. D **88**, 054012 (2013).
- [50] S. H. Kim, A. Hosaka, and H. C. Kim, Phys. Rev. D **90**, 014021 (2014).
- [51] J. Beringer *et al.*, (Particle Data Group), Phys. Rev. D **86**, 010001 (2012).
- [52] K. Nakamura *et al.*, (Particle Data Group), J. Phys. G **37**, 075021 (2010).
- [53] T. Corthals, J. Ryckebusch, and T. Van Cauteren, Phys. Rev. C **73**, 045207 (2006).
- [54] L. De Cruz, J. Ryckebusch, T. Vrancx, and P. Vancraeyveld, Phys. Rev. C **86**, 015212 (2012).
- [55] V. L. Kashevarov, L. Tiator, and M. Ostrick, Bled Workshops Phys. **18**, 1 (2017).
- [56] I. S. Barker, A. Donnachie and J. K. Storrow, Nucl. Phys. B **95**, 347 (1975).
- [57] C. G. Fasano, F. Tabakin and B. Saghai, Phys. Rev. C **46**, 2430 (1992).